JOURNAL OF VIROLOGY, Aug. 2003, p. 9084–9089 Vol. 77, No. 16
0022-538X/03/$08.00+0 DOI: 10.1128/JVI.77.16.9084–9089.2003

Recombinant Avian Infectious Bronchitis Virus Expressing a Heterologous Spike Gene Demonstrates that the Spike Protein Is a Determinant of Cell Tropism

Rosa Casais, Brian Dove, David Cavanagh, and Paul Britton*

Division of Molecular Biology, Institute for Animal Health, Compton Laboratory, Compton,

overlaps the N-terminal end of the S gene by 50 nucleotides (nt). (iii) The region of the S gene corresponding to the S2 subunit encodes part of the ectodomain, the transmembrane, and cytoplasmic tail regions, of which the latter are responsible for incorporation of the S glycoprotein into coronavirus particles (12).

Sequence analysis of the M41-CK S gene identified 72 nt differences from the Beau-R S gene sequence, of which 50 represented nonsynonymous substitutions and 22 represented synonymous substitutions, resulting in a total of 47 amino acid differences between the two S glycoproteins. The last nonsynonymous substitution results in a premature stop codon within the M41 S gene, so that the M41-CK S glycoprotein is nine amino acids shorter than the Beaudette protein. Apart from the loss of the nine amino acids, there were no other amino acid differences between the cytoplasmic domains of the two viruses. Overall, the primary translation products of the two S genes are 1,153 and 1,162 amino acids in size for M41-CK and Beau-R, respectively, representing an identity of 95.2% between the two S proteins. Comparison of the replicase sequence that overlaps the S gene sequence showed that there is only one synonymous mutation, with no mutations between the S-gene transcription-associated sequence (TAS) and the initiation codon of the S gene (Fig. 1).

A chimeric S gene, consisting of the signal sequence, ectodomain, and transmembrane regions derived from M41-CK and the cytoplasmic tail domain from Beau-R, was produced. The last 137 nt of the Beaudette S gene, comprising the cytoplasmic domain, were retained to maintain any interaction of the S protein C-terminal domain with the other Beaudette-derived proteins. The transmembrane regions are identical between the two S glycoproteins; therefore, the mature form of the chimeric S glycoprotein only differed in the ectodomain, derived from M41-CK, compared to the Beaudette S glycoprotein. A plasmid, pFRAG3-M41S, contain(S-genne3gFRAG3-M41r(8a(cont,30.4(th-is.)-494.9(Compa-494.9etwJed)-32ycopro-) eid)-32yce)

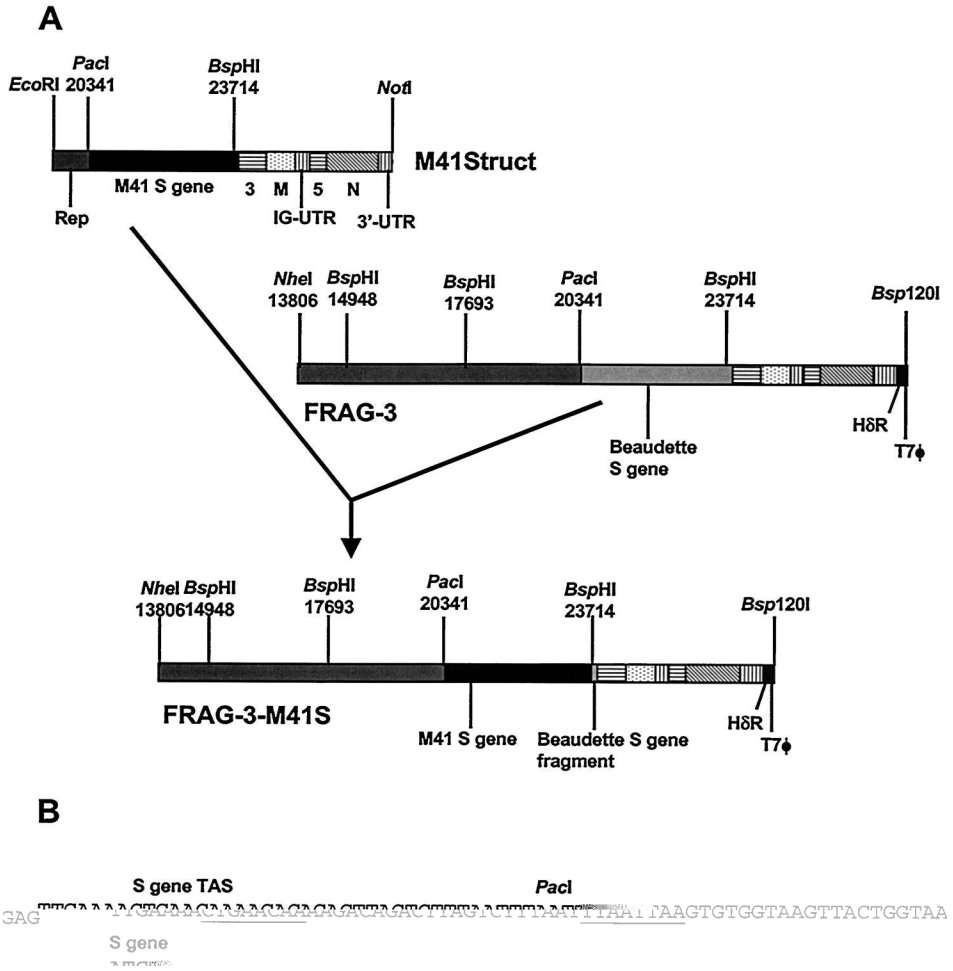

FIG. 2. Schematic diagram for the construction of the chimeric S gene and production of a full-length IBV cDNA. (A) Replacement of the ectodomain region of the Beaudette S gene by the corresponding sequence from IBV M41 for construction of FRAG-3-M41S. (B) Junction of the S gene sequences at the *Pac*I and *Bsp*HI restriction sites with the intervening sequence derived from M41. The nucleotides in bold correspond to the signal and transmembrane sequences, respectively. (C) Schematic diagram of the BeauR-M41(S) full-length cDNA composed of FRAG-1, FRAG-2, and FRAG-3-M41S.

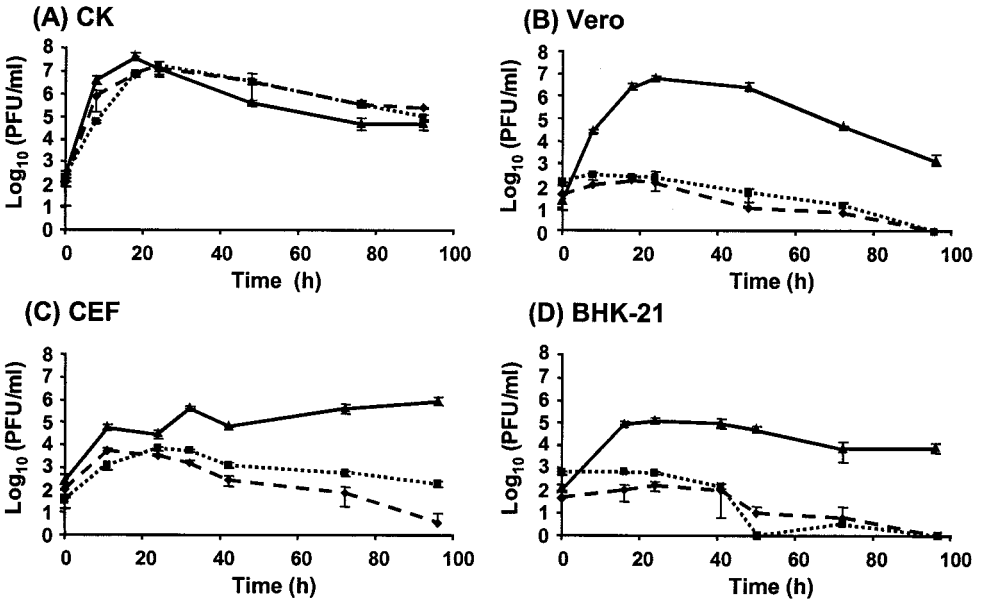

FIG. 3. Growth profiles of the three IBVs on four cell types. Cells were infected with 1.5×10^6 PFU of each IBV, and cell medium was analyzed for progeny virus by plaque titration assay on CK cells 0 to 96 h postinfection. The panels show the growth patterns of Beau-R (solid line with triangle), M41-CK (dashed line with diamond), and BeauR-M41(S) (dotted line with square) on CK cells (A), Vero cells (B), CEF cells (C), and BHK-21 cells (D).

Beau-R, M41-CK, and BeauR-M41(S) were used to infect four different cell types, and the titer of progeny virus was determined over a 96-h period. All three viruses displayed similar growth profiles on CK cells (Fig. 3A). Progeny virus was detectable 8 h postinfection, with peak titers of 10^7 PFU/ml at 18 to 24 h postinfection, showing that the three viruses replicated to a similar extent in CK cells irrespective of the origin of the S gene. The growth profiles of the three viruses were then analyzed in CEF cells, previously shown to support the growth of 10 different IBV strains, including M41, which produced 1000-fold less virus than Beaudette (20), and on two mammalian cell lines, Vero and BHK-21. Only two strains of IBV, including Beaudette, had been demonstrated to grow on BHK-21 cells (20).

Analysis of the growth profiles of the three viruses in Vero, CEF, and BHK-21 (Fig. 3B to D) showed that only Beau-R replicated to any significant extent in the different cells, usually with maximum titer by 24 h postinfection. In Vero cells, Beau-R replicated to a titer of 10^7 PFU/ml at 24 h postinfection, while BeauR-M41(S) and M41-CK showed 10^4-fold-lower titers (Fig. 3B). Both M41-CK and BeauR-M41(S) barely increased in titer above the titer observed at time zero and after 30 h postinfection showed little evidence for production of new infectious virus.

In CEF cells, M41-CK and BeauR-M41(S) initially grew, but to a lower level than observed for Beau-R. The Beau-R titer increased approximately 1,800-fold by 30 h postinfection, whereas the titers for M41-CK and BeauR-M41(S) only increased approximately 15-fold over the same time period (Fig. 3C). However, after 30 h postinfection, only the titer of Beau-R continued to increase, while the titers of M41-CK and BeauR-M41(S) decreased.

Similarly, Beau-R replicated to a titer of 10^5 PFU/ml at 24 h postinfection on BHK-21 cells, while BeauR-M41(S) and M41-CK showed more than 10^2-fold-lower titers with little to no growth compared to the titers at time zero (Fig. 3D). This observation corroborates the results of Otsuki et al. (20), who demonstrated that Beaudette but not M41 replicated on BHK-21 cells. Our results demonstrated that BeauR-M41(S) had the same tropism as M41-CK on all four cell types.

The growth experiments represented the measurement of progeny virus, following a single infection, over a time period. Therefore, we decided to investigate the possibility that serial passage might result in amplification following adaptation or selection of progeny virus in the different cell types. The four cell types were infected with the three viruses at 2×10^7 PFU (P_1), and after 24 h postinfection, progeny virus was serially passaged twice (P_2 and P_3). Total cellular RNA was extracted from the cytoplasm of P_1 to P_3 cells and analyzed by reverse transcription (RT)-PCR using oligonucleotides located in the N gene and 3′ untranslated region. Detection of an RT-PCR product of 666 bp for Beau-R and BeauR-M41(S) or 481 bp for M41-CK was indicative of IBV replication.

Analysis of the RT-PCR products from RNA isolated from P_1 to P_3 CK cells infected with Beau-R, M41-CK, and BeauR-M41(S) confirmed that all three viruses were serially passaged on CK cells (Fig. 4A). RT-PCR analysis of RNA derived from Vero cells showed that only Beau-R was passaged on Vero cells (Fig. 4B). Although IBV RNA was detected in P_1 cells infected with M41-CK and BeauR-M41(S), there was no evidence of IBV-derived RNA following passage of the viruses in P_2 and P_3 Vero cells (Fig. 4B). Detection of M41-CK and BeauR-M41(S)-derived RNA in P_1 Vero cells may have resulted from (i) the virus inoculum, indicating that neither virus replicated in Vero cells, or (ii) low levels of replication in P_1 Vero cells, resulting in low titers of progeny virus, so that

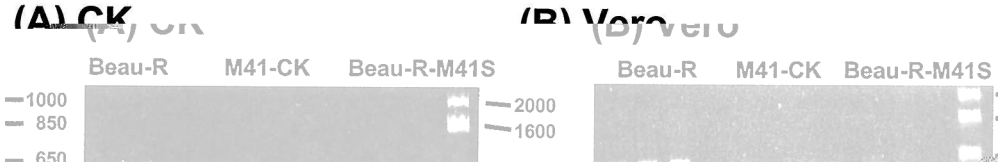

FIG. 4. Detection of IBV by RT-PCR following passage of Beau-R, M41-CK, or BeauR-M41(S) on CK, Vero, CEF, or BHK-21 cells. Cells (P_1) were infected with 2×10^7 PFU of each virus, and 24 h postinfection any progeny viruses were passaged twice (P_1 to P_3). Total cellular RNA was isolated from the IBV-infected cells and used for RT-PCR analysis; an RT-PCR product of 666 bp corresponded to detection of Beau-R- and BeauR-M41(S)- derived RNA, and a product of 481 bp corresponded to detection of M41-CK-derived RNA. The RT-PCR products detected following passage (P_1 to P_3) of Beau-R, M41-CK, or BeauR-M41(S) on CK (A), Vero (B), CEF (C), or BHK-21 (D) cells were analyzed on 1% agarose gels.

resultant amounts of RNA in P_2 and P_3 cells were below the threshold of detection by RT-PCR.

Analysis of RNA isolated from CEF cells showed that all three viruses were detected in P_1-P_2 cells, indicating that the viruses grew in this cell type (Fig. 4C). This confirmed the results obtained from the growth experiment (Fig. 3C), with the RT-PCR analysis detecting growth of the three viruses in the initial 24-h period. The reason for the decline in growth of M41-CK and BeauR-M41(S) after 30 h postinfection is not known (Fig. 3C).

RT-PCR analysis of RNA isolated from BHK-21 cells infected with the three viruses showed that only Beau-R could be passaged on this cell type (Fig. 4D). The analysis showed the presence of IBV-derived RNA in P_1 BHK-21 cells infected with all three viruses. There was no evidence that M41-CK was passaged beyond P_1 on BHK-21 cells. Although BeauR-M41(S) was detected in P_1 BHK-21 cells, the amount detected at P_2 was lower, and no IBV RNA was detected in P_3 cells. Overall, these results demonstrated that exchange of the ectodomain of the S protein resulted in the loss of the ability of Beau-R to establish a successful infectious cycle in Vero, CEF, and BHK-21 cells.

We have used our IBV reverse genetics system to produce a rIBV, BeauR-M41(S), consisting of the Beaudette genome but with the ectodomain region of the S gene replaced with the corresponding sequence from M41-CK. Our results demonstrated that BeauR-M41(S) had the growth characteristics of M41-CK on four cell types and that replacement of only the ectodomain of the Beaudette S glycoprotein with the M41-CK homologue resulted in the altered growth characteristics of Beau-R. The results demonstrated that the IBV S protein plays a major role in the cell tropism of the virus.

This work was supported by the Commission of the European Communities specific RTD program Quality of Life and Management of Living Resources, QLK2-CT-1999-00002, the Department of Environment, Food and Rural Affairs, project code OD0712, and the Biotechnology and Biological Sciences Research Council.

REFERENCES

1. **Britton, P.** 1991. Coronavirus motif. Nature **353:**394.
2. **Casais, R., V. Thiel, S. G. Siddell, D. Ca anagh, and P. Britton.** 2001. Reverse genetics system for the avian coronavirus infectious bronchitis virus. J. Virol. **75:**12359–12369.
3. **Ca anagh, D.** 2001. A nomenclature for avian coronavirus isolates and the question of species status. Avian Pathol. **30:**109–115.
4. **Ca anagh, D., K. Ma ditt, M. Sharma, S. E. Drur , H. L. Ains orth, P. Britton, and R. E. Gough.** 2001. Detection of a coronavirus from turkey poults in Europe genetically related to infectious bronchitis virus of chickens. Avian Pathol. **30:**365–378.
5. **Ca anagh, D., K. Ma ditt, D. B. B. Welchman, P. Britton, and R. E. Gough.** 2002. Coronaviruses from pheasants (*Phasianus colchicus*) are genetically closely related to coronaviruses of domestic fowl (infectious bronchitis virus) and turkeys. Avian Pathol. **31:**81–93.
6. **Ca anagh, D., and S. Naqi.** 2003. Infectious bronchitis, p. 101–119. *In* Y. M.

Saif, H. J. Barnes, J. R. Glisson, A. M. Fadly, L. R. McDougald, and D. E. Swayne (ed.), Diseases of poultry, 11th ed. Iowa State University Press, Ames.

7. **Cook, J. K., J. Chesher, W. Ba endale, N. Green ood, M. B. Huggins, and S. J. Orbell.** 2001. Protection of chickens against renal damage caused by a nephropathogenic infectious bronchitis virus. Avian Pathol. **30:**423–426.
8. **Darb shire, J. H., J. G. Ro ell, J. K. A. Cook, and R. W. Peters.** 1979. Taxonomic studies on strains of avian infectious bronchitis virus using neutralisation tests in tracheal organ cultures. Arch. Virol. **61:**227–238.
9. **Das Sarma, J., L. Fu, J. C. Tsai, S. R. Weiss, and E. La i.** 2000. Demyelination determinants map to the spike glycoprotein gene of coronavirus mouse hepatitis virus. J. Virol. **74:**9206–9213.
10. **De Groot, R. J., W. Lu tjes, M. C. Hor inek, B. A. M. Van der Zeijst, W. J. M. Spaan, and J. A. Lenstra.** 1987. Evidence for a coiled-coil structure in the spike proteins of coronaviruses. J. Mol. Biol. **196:**963–966.
11. **de Vries, A. A. F., M. C. Hor inek, P. J. M. Rottier, and R. J. de Groot.** 1997. The genome organisation of the Nidovirales: similarities and differences between arteri-, toro- and coronaviruses. Semin. Virol. **8:**33–47.
12. **Godeke, G. J., C. A. de Haan, J. W. Rossen, H. Vennema, and P. J. Rottier.** 2000. Assembly of spikes into coronavirus particles is mediated by the carboxy-terminal domain of the spike protein. J. Virol. **74:**1566–1571.
13. **Hisco , J. A., T. Wurm, L. Wilson, P. Britton, D. Ca anagh, and G. Brooks.** 2001. The coronavirus infectious bronchitis virus nucleoprotein localizes to the nucleolus. J. Virol. **75:**506–512.
14. **Koch, G., L. Hartog, A. Kant, and D. J. an Roo elaar.** 1990. Antigenic domains of the peplomer protein of avian infectious bronchitis virus: correlation with biological function. J. Gen. Virol. **71:**1929–1935.
15. **Kuo, L., G. J. Godeke, M. J. Raamsman, P. S. Masters, and P. J. Rottier.** 2000. Retargeting of coronavirus by substitution of the spike glycoprotein ectodomain: crossing the host cell species barrier. J. Virol. **74:**1393–1406.
16. **Lai, M. M., and D. Ca anagh.** 1997. The molecular biology of coronaviruses. Adv. Virus Res. **48:**1–100.
17. **Luo, Z., A. M. Matthe s, and S. R. Weiss.** 1999. Amino acid substitutions within the leucine zipper domain of the murine coronavirus spike protein cause defects in oligomerization and the ability to induce cell-to-cell fusion. J. Virol. **73:**8152–8159.
18. **Luo, Z. L., and S. R. Weiss.** 1998. Roles in cell-to-cell fusion of two conserved hydrophobic regions in the murine coronavirus spike protein. Virology **244:**483–494.
19. **Na as, S., S. H. Seo, M. M. Chua, J. D. Sarma, E. La i, S. T. Hingle , and S. R. Weiss.** 2001. Murine coronavirus spike protein determines the ability of the virus to replicate in the liver and cause hepatitis. J. Virol. **75:**2452–2457.
20. **Otsuki, K., K. Noro, H. Yamamoto, and M. Tsubokura.** 1979. Studies on avian infectious bronchitis virus (IBV). II. Propagation of IBV in several cultured cells. Arch. Virol. **60:**115–122.
21. **Phillips, J. J., M. M. Chua, E. La i, and S. R. Weiss.** 1999. Pathogenesis of chimeric MHV4/MHV-A59 recombinant viruses: the murine coronavirus spike protein is a major determinant of neurovirulence. J. Virol. **73:**7752–7760.
22. **Sánche , C. M., A. Ie eta, J. M. Sánche -Morgado, S. Alonso, I. Sola, M. Balasch, J. Plana-Durán, and L. Enjuanes.** 1999. Targeted recombination demonstrates that the spike gene of transmissible gastroenteritis coronavirus is a determinant of its enteric tropism and virulence. J. Virol. **73:**7607–7618.
23. **Schul e, B., D. Ca anagh, and G. Herrler.** 1992. Neuraminidase treatment of avian infectious bronchitis coronavirus reveals a hemagglutinating activity that is dependant on sialic acid containing receptors on erythrocytes. Virology **89:**792–794.
24. **Siddell, S. G.** 1995. The *Coronaviridae*, p. 1–10. *In* S. G. Siddell (ed.), The *Coronaviridae.* Plenum, New York, N.Y.